Introduction

Understanding how energy is transmitted and received by Ground Penetrating Radar antennas is crucial to many areas of the industry: antenna design, data processing and inversion algorithms, usage of antennas in GPR surveys, and interpretation of GPR responses. The radiation characteristics of antennas are usually investigated by studying the radiation patterns and directivity. For GPR antennas it is important to study these characteristics when the antenna is in different environments that would typically be encountered in GPR surveys. This is because interactions between the antenna and the environment change the way in which the antenna behaves. However, directly measuring antenna radiation patterns in such environments presents many practical difficulties, which has prompted numerical simulations of GPR antenna radiation patterns. Although simple and more complex antennas have been modelled in free-space, and simple antennas have been modelled in realistic environments, there have been very limited studies that combine real GPR antenna models with realistic environments.

This paper presents a numerical investigation of the radiation characteristics of a high-frequency GPR antenna in a realistic environment that incorporates a heterogeneous soil. The first part of the paper describes the 3D Finite-Difference Time-Domain (FDTD) antenna model and the soil model. Then analyses of E- and H-plane directivity patterns from the antenna model over a heterogeneous soil are presented and compared with patterns in a lossless dielectric environment.

Antenna modelling

All of the simulations conducted for this research used gprMax3D which is part of gprMax, a suite of electromagnetic wave simulators based on the FDTD method. gprMax (http://www.gprmax.com/) is freely available software that was written by Giannopoulos (2005) originally in 1996, and has since developed into a mature application that has been successfully used by a number of researchers (Galagedara et al., 2005; Jeannin et al., 2006; Lopera and Milisavljevic, 2007; Soldovieri et al., 2007). The simulations included a model of the antenna that is representative of a commonly used high-frequency GPR antenna – a Geophysical Survey Systems, Inc. (GSSI) 1.5 GHz antenna. The antenna model includes all of the main features and geometry of the real antenna. Details of the antenna model development and the subsequent initial validation can be found in Warren and Giannopoulos (2011). Figure 1a shows the FDTD mesh of the antenna with skid plate removed. A spatial discretisation of $\Delta x = \Delta y = \Delta z = 1$ mm was chosen as a good compromise between accuracy and computational requirements. The Courant Friedrichs Lewy (CFL) condition was enforced which resulted in a time-step of $\Delta t = 1.926$ ps.

Soil modelling

Advanced and innovative developments were made to gprMax to create soils with realistic dielectric and geometrical properties. A semi-empirical model, initially suggested by Dobson et al. (1985), was used to describe the dielectric properties of the soil. The model relates relative permittivity of the soil to bulk density, sand particle density, sand fraction, clay fraction and water volumetric fraction. The real and imaginary parts of this semi-empirical model can be approximated using a multi-pole Debye function plus a conductive term. In gprMax a recursive convolution based method was used to express dispersive properties as apparent current density sources (Giannakis and Giannopoulos, 2014). A major advantage of this implementation is that it creates an inclusive susceptibility function that holds, as special cases, Debye, Drude and Lorenz materials.

Fractals are scale invariant functions which can express the earths topography for a wide range of scales in sufficient detail (Turcotte, 1987). Using this approach, a more realistic soil model with a stochastic distribution of the aforementioned parameters was created. Figure 1b shows a FDTD mesh in gprMax featuring the antenna model, and a soil model with realistic dielectric and geometrical properties.

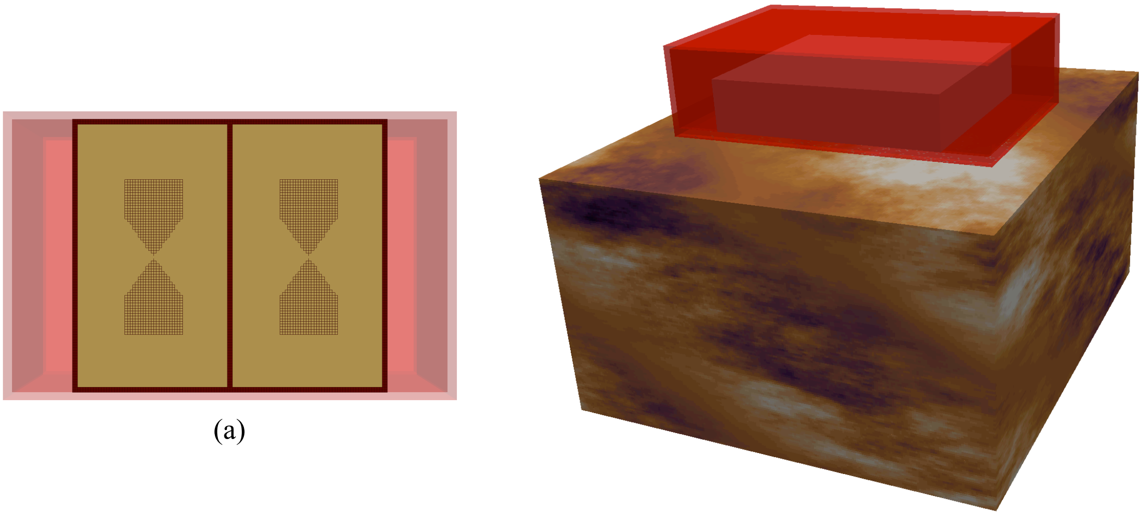

(a) (b)

Figure 1 *FDTD meshes: (a) representative of a GSSI 1.5 GHz antenna; and (b) showing the antenna over a heterogeneous soil, modelled using a stochastic distribution of soil parameters.*

Antenna patterns in lossless, lossy, and heterogeneous environments

Traditionally antenna patterns are plotted at a specific single frequency, however this is of limited use when analysing the overall performance of an UWB GPR antenna. In this paper a more suitable metric that calculates the transmitted energy at a specific observation point, given by (1), has been used. It was originally proposed by Diamanti and Annan (2013).

$$E_{tot}(r,\theta) = \sum_{t}^{T} \frac{E(r,\theta)^2}{Z} \tag{1}$$

where E_{tot} is the total energy at a specific radius r and angle θ; the summation is made over a time-domain response; E is the electric field value at a given radius r and angle θ; and Z is the electromagnetic impedance of the medium.

Figure 2 presents a comparison of the H-plane patterns of the antenna in two environments: a lossless half-space with a relative permittivity of 7, and a heterogeneous soil with sand fraction 0.9, clay fraction 0.1, sand particle density 2.0 g/cm^3, bulk density of 2.66 g/cm^3, and a volumetric water fraction ranging from 0.02 to 0.05. As an indication of the relative permittivity variation of the soil, the static or zero-frequency parts of relative permittivity range from 5.77 to 8.51 with 50 discrete values. Fractal weightings for the x, y, z directions were chosen as 1.5, 1.5, 0.375, with the lower weighting in the z direction used to create more realistic layering. The asymmetry present in the H-plane pattern is due to the offset between the T_x and R_x elements in the antenna. The stronger part of the back or air lobe corresponds to the T_x location in the antenna. As expected there is more attenuation (up to 3 dB) in the pattern with the dispersive heterogeneous soil than the lossless half-space. The attenuation is largest in the main lobe of the pattern and less so at shallow angles. This behaviour could be attributed to the FDTD antenna model not capturing the way in which lateral waves propagate from the real antenna. It has been previously observed by Warren and Giannopoulos (2015) in numerical models that included an antenna model and dispersive emulsions.

Figure 3 presents the same comparison as Figure 2 but with E-plane patterns. The antenna geometry in symmetric in the E-plane which results in a symmetric E-plane pattern. Similar differences exist in the strength of directivity of the patterns between the two environments.

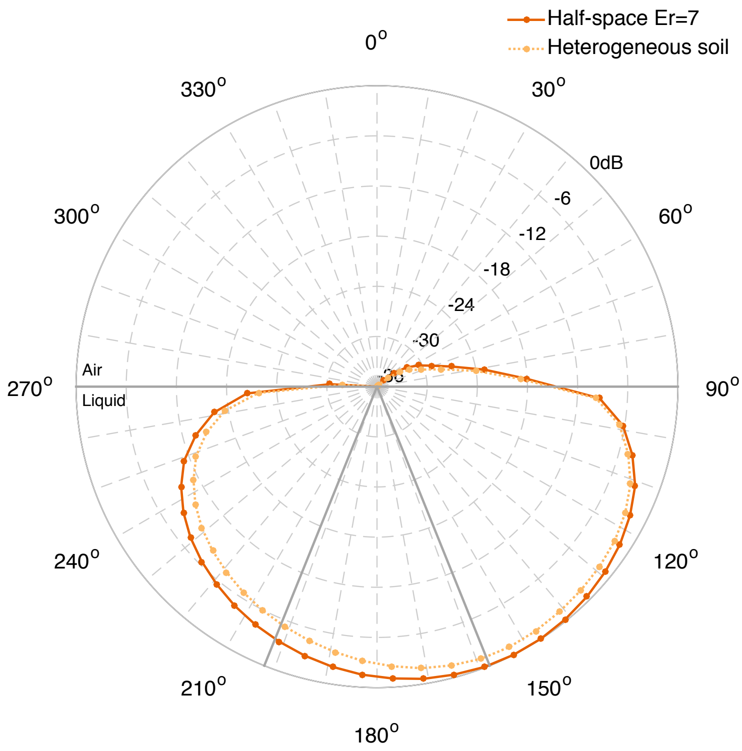

Figure 2 H-plane directivity patterns of the GSSI 1.5GHz antenna model over a lossless dielectric half-space of relative permittivity 7, and over a dispersive heterogeneous soil.

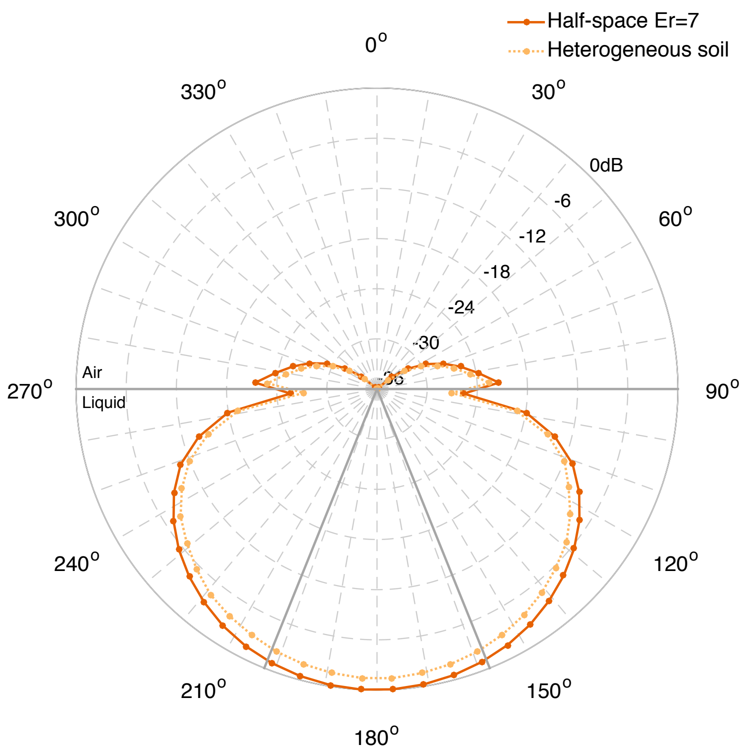

Figure 3 E-plane directivity patterns of the GSSI 1.5GHz antenna model over a lossless dielectric half-space of relative permittivity 7, and over a dispersive heterogeneous soil.

Conclusions

The investigation of radiation characteristics of an antenna makes it possible to develop a better understanding of how the antenna radiates and receives energy. An advanced modelling toolset that enables detailed models of GPR antennas to be used in realistic environments that include models of heterogeneous soils has been developed. In this initial investigation small differences in the directivity of the antenna between a lossless dielectric environment and a more realistic environment featuring a heterogeneous soil model have been observed. These findings are part of an on-going full parametric study incorporating a range of different soils, fractal weightings and also the inclusion of rough surface modelling.

References

Diamanti, N., and Annan, A. P. [2013] Characterizing the energy distribution around GPR antennas. *Journal of Applied Geophysics*, **99**, 83– 90.

Dobson, M. C., Ulaby, F. T., Hallikainen, M. T., and El-Rayes, M. A. [1985] Microwave dielectric behavior of wet soil-part ii: Dielectric mixing models *Geoscience and Remote Sensing, IEEE Transactions on*, **1**, 35–46.

Galagedara, L., Redman, J., Parkin, G., Annan, A., and Endres, A. [2005] Numerical modeling of GPR to determine the direct ground wave sampling depth. *Vadose Zone Journal*, **4**, 1096–1106.

Giannakis, I., and Giannopoulos, A. [2014] A novel piecewise linear recursive convolution approach for dispersive media using the finite-difference time-domain method *Antennas and Propagation, IEEE Transactions on*, **62**(5), 2669–2678.

Giannopoulos, A. [2005] Modelling Ground Penetrating Radar by GprMax *Construction and Building materials*, **19**(10), 755–762.

Jeannin, M., Garambois, S., Gregoire, C., and Jongmans, D. [2006] Multiconfiguration GPR measurements for geometric fracture characterization in limestone cliffs (Alps) *Geophysics*, **71**, B85.

Lopera, O., and Milisavljevic, N. [2007] Prediction of the effects of soil and target properties on the antipersonnel landmine detection performance of ground-penetrating radar: A Colombian case study. *Journal of Applied Geophysics*, **63**(1), 13–23.

Soldovieri, F., Hugenschmidt, J., Persico, R., and Leone, G. [2007] A linear inverse scattering algorithm for realistic GPR applications. *Near Surface Geophysics*, **5**(1), 29–42.

Turcotte, D. L. [1987] A fractal interpretation of topography and geoid spectra on the Earth, Moon, Venus and Mars. *Journal of Geophysics*, **94**(B4), E597–E601.

Warren, C., and Giannopoulos, A. [2011] Creating FDTD models of commercial GPR antennas using Taguchi's optimisation method. *Geophysics*, **76**(37), G37–G47.

Warren, C., and Giannopoulos, A. [2015] Experimental and modelled performance of a Ground Penetrating Radar antenna in lossy dielectrics. *Selected Topics in Applied Earth Observations and Remote Sensing, IEEE Journal of*, (in press)